Experimental microscopic study of inner pores of calcareous sand

C.-Q. Zhu*[1], X.-Z. Wang[1], R. Wang[1], H.-Y. Chen[2] and Q.-S. Meng[1]

Microscopic experiments were performed on the inner pores of calcareous sand particles to ascertain the special mechanical properties of calcareous sand. A femtosecond laser was used to cut the calcareous sand particles to obtain cross-sections of particle. The micrographs of the inner pores of the sand particles were taken with a three-dimensional video microscopic visualiser. The parameters of the pores were analysed through the micrograph processing with MATLAB. The results show that calcareous sand has relatively low surface porosity. The surface porosities of particles with pore diameter >2 mm and those in the range of 1–2 mm are 0·66 and 1·07% respectively. Based upon the number of pores, the distribution characteristics of the pores show that there are fewer macropores but more micropores in the sand. In terms of the area of pores, micropores occupy a smaller proportion than macropores. It was found that 65% of the pores have area $<1\ \mu m^2$, and 55% or more of them are equiaxed pores.

Keywords: Inner pore, Pore characteristic, Femtosecond laser, Image processing, Calcareous sand

Introduction

Calcareous sand from the Nansha Islands, South China Sea, is a special marine biogenic material that contains >97% calcium carbonate.[1,2] According to previous studies, calcareous sand exhibited significantly different characteristics from those of terrigenous sand because of the presence of inner pores at conventional mechanical testing, including particle crushing behaviour, saturation difficulty and high compressibility.[3,4,5] The in depth studies of the inner pores of calcareous sand and discovery of its distribution characteristics greatly improved the understanding of the relationship between the microscopic pores and their macromechanical properties. These studies include the analysis of their mechanical properties and research related to calcareous sand.[6,7]

To date, the conventional method for the microscopic study of pores usually compresses certain specific substances into a medium under a certain pressure to analyse the pore characteristics. An example is mercury porosimetry, which injects mercury into a medium under a certain pressure.[8] Consequently, the size of various pores can be calculated based on the volume of the injected mercury.[9] However, it is difficult to measure the size of the pores, since the injection of mercury into both sealed and partially sealed pores in calcareous sand is challenging.

Methods with adoption of nuclear magnetic resonance and gas adsorption are used to inject either water or gas into the pores of a medium under a certain pressure. The pores are then measured by analysing the interaction of the water or gas in the pores and pore walls. Although the infiltration characteristic of water and inert gases are stronger than that of mercury, it is difficult to measure the sealed pores of the medium. Similarly, when the samples are compressed using these methods, a rock medium with a lower degree of strength can be partially cracked or damaged at a certain pressure. Therefore, the test results are subjected to large errors or mistakes due to release of pores into the medium.

Flat cross-sections of particles are needed to study the characteristics of the inner pores of calcareous sand particles. During this process, the pores and their distribution should not be destroyed, and their original characteristics should be preserved. Destruction of both surrounding medium and the original form of the pores occurs, even with appearance of cracks, due to surrounding stress on the pores when applying mechanical/manual cutting or manual grinding of the samples. Especially, this effect is commonly observed for media with low degrees of strength. Meanwhile, tiny pores can be easily squeezed and filled while using a powdered medium, and thus became vulnerable. In addition, these methods are difficult to implement for cutting and grinding smaller particles.

From above analysis, conventional experimental methods cannot be used to effectively study the characteristics of the inner pores of calcareous sand. Therefore, in this study, a femtosecond laser cold cutting method is used to cut the calcareous sand particles to produce sample cross-sections. As a result, the inner

[1]State Key Laboratory of Geomechanics and Geotechnical Engineering, Institute of Rock and Soil Mechanics, Chinese Academy of Sciences, Wuhan 430071, China
[2]Shanghai Geotechnical Investigations and Design Institute Co. Ltd, Shanghai 200032, China

*Corresponding author, email cqzhu@whrsm.ac.cn

Received 15 September 2013; accepted 12 December 2013
DOI 10.1179/1432891714Z.000000000408

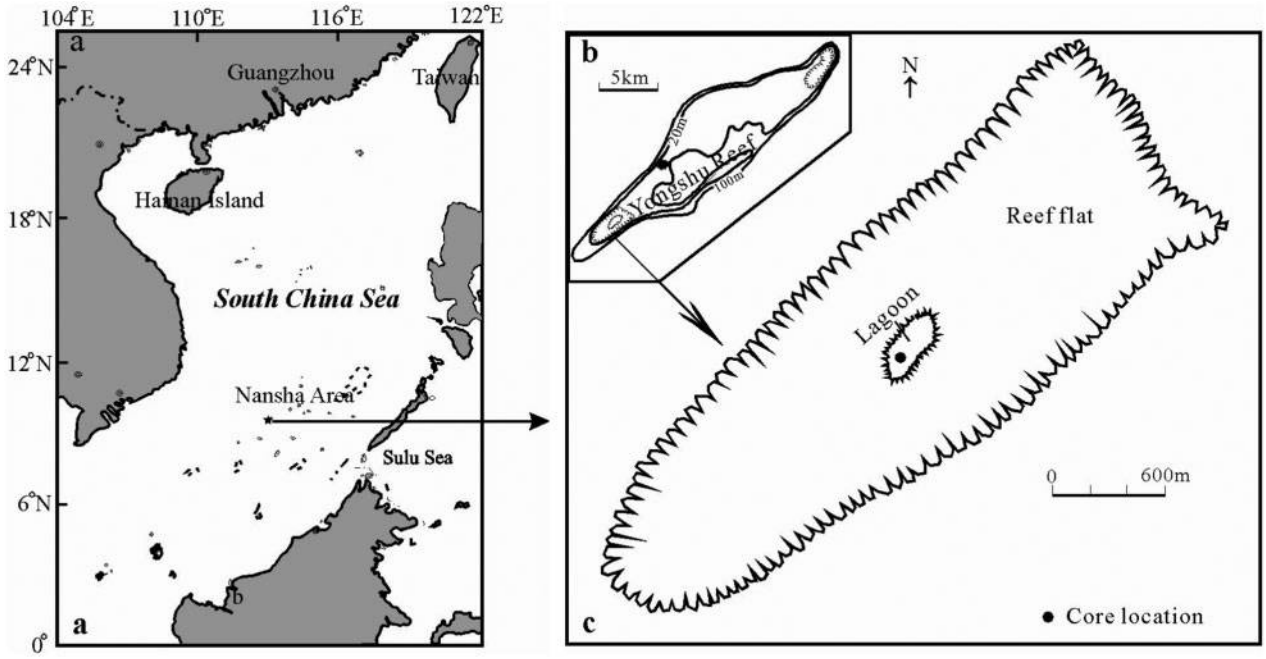

1 ***a*** **map showing location of Yongshu Reef, Nansha Islands, South China Sea and** ***b*** **location of samples on Yongshu Reef[10]**

pores of calcareous sand are exposed and micrographs of these pores are obtained. The images are processed with MATLAB to analyse the main characteristic parameters of the inner pores of the particles. Thereafter, further investigation of the inner pores of calcareous sand is conducted using statistical test methods.

Sample preparations

In this study, a femtosecond laser was used to cut calcareous sand particles to maintain the original structure and appearance of their inner pores. There are three major advantages with the femtosecond method: extremely short operation time scale (i.e. $\sim 10^{-15}$ s); extremely high instantaneous power that reaches up to 100 trillion watts; and extremely small spatial region of focus that can be smaller than the diameter of a human hair, and thus, the strength of the electromagnetic field is many times stronger than the force of the electrons around the nucleus.[11] In light of these features, when a femtosecond laser is applied to calcareous sand particles, the areas surrounding the incision become plasmas and are affected minimally. This allows a sharp and clean cut appearance, which ensures that the inner pores of the calcareous sand particles are not destroyed.

Experimental instrument

A Ti:sapphire mode locked laser manufactured by Spectra-Physics was used. The laser's main parameters are as follows: single pulse energy, $E=1{\cdot}2$ mJ; frequency, $f=1$ kHz; central wavelength $\lambda_0=800$ nm; bandwidth, $\Delta\lambda=40$ nm; pulse width, $T=50$ fs; light spot diameter, $\Phi=8$ mm; and a cut width ranging from 150 to 200 μm.

Sample cutting

Uncemented calcareous sand particles were sampled from a lagoon in the Yongshu Reef, Nansha Islands, South China Sea (Fig. 1). The particles were washed with water and dried. Considering the small size of the particles, they were glued onto glass plates to prevent from rolling or spattering during the cutting process. The dimensions of the glass plates are $1{\cdot}5 \times 5$ cm. The particles were lined up in a row close to the edge in the longitudinal direction of the glass plates, as shown in Fig. 2, for operation of the laser.

Image acquisition

Experimental instrument

In this experiment, a three-dimensional (3D) video microscopic visualiser, KH-300, was used, along with equipments for imaging and storing images. This instrument is capable of performing auto-identification of the strengthening of the inner pore edges of a cross-section. The magnification of colour images in this experiment was 400, with the field of view of $\sim 0{\cdot}8 \times 1{\cdot}1$ mm, equivalently 1600×1200 pixels.

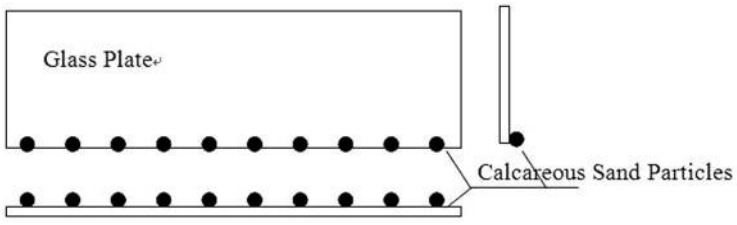

2 Schematic diagram of laser cutting of calcareous sand particles

Image analysis

First, the colour images were converted to binary ones with binarisation processing. Under the same resolution, grey scale threshold selection was the key for determining whether the binary images could reflect the structures of the pores. Generally, there are two threshold selection methods: a visual method and a procedural method. The former one was used in this study.

The original micrographs were true colour images. Initially, these images were converted into greyscale images, i.e. the colour was removed from the images and only the intensity information was retained. In such format, the storage of grey images only requires one data matrix. Each element of the matrix represents the grey value of the corresponding pixel. Double data type was chosen for the greyscale images with time domains [0, 1].

In the visual method, the edges of the relatively larger pores were inspected visually, and statistics associated with their pixel values were collected to find the true pixel values at the edges under certain resolution conditions. Thereafter, the pixel values were set to a binarisation threshold value. Pixel points below the threshold were redefined as 0, while those that exceeded the threshold were redefined as 1. By doing so, the images were converted into binary ones (i.e. images that contain only 0 and 1). The threshold value was revised by comparing the binarised image to the original image in order to obtain an optimal threshold value under a certain resolution. A number of previous studies have demonstrated that the thresholds should be identical under the same resolution and experimental conditions. Therefore, in this study, the same threshold was chosen for the same set of photos in both the experiment and analysis.

The images were analysed using MATLAB image processing toolbox. Digital processing was performed on micrographs, and digital matrices with values of 0 and 1 were obtained through binarisation. In order to facilitate the pore distribution and calibration, the binarised images were reversed, resulting in a new pixel value of 0 instead of 1 at original images and vice versa (Fig. 3).

Figure 4*a* shows an example of a binarised image before storage, and Fig. 4*b* shows the data matrix stored. In order to quantify the pores in the images, the pores had to be marked individually. With the built in image processing toolbox in MATLAB, pores were then labelled following binarisation, as shown in Fig. 4*c*.

An in-house programme was written for image processing to calculate the circumference (pixels) of the projecting contour of the pores, field area (pixels) of the projecting contour, as well as the parameters of the related pores. The procedure is presented as follows:

(i) a 'four-neighbourhood' search method was used (Fig. 5) to identify and label the pores with image processing toolbox of MATLAB
(ii) the resulting circumference/area matrix of each pore, D (2, n), was defined, where n is the number of pores
(iii) each pore was analysed for the resulting image matrix; for the ith pore, D ($2i-1$) was assigned to all pores with a pixel value of i in the image; the operators were found using the built in 'Candy' boundary in MATLAB in order to measure the circumference of the pore, and D ($2i$) was assigned to the value.
(iv) the binarised image was reviewed to determine the area and circumference of each pore.

The experimental picture was digitised into a 1600×1200 pixel image. The physical size of the picture is $423{\cdot}3 \times 317{\cdot}5$ mm. The magnification is $\times 400$, and the physical resolution represented by each pixel δ was

$$\delta = \frac{317{\cdot}5 \times 1000}{1200 \times 400} = 0{\cdot}6614583\ \mu\text{m}$$

According to the physical value of each pixel, the circumference (pixels) and area (pixels) of the pores in the particle cross-section were converted to a physical circumference value (μm) and a physical area value (μm^2).

Analysis of results

Surface porosity

The surface porosity n_w, which is usually defined as the ratio of the pores in calcareous sand particles to a complete cross-section, is as follows

$$n_w = \frac{G_w}{G_T} \times 100\%$$

where G_w is the cross-sectional area of all pores, and G_T is the total area of the entire area being analysed.

The scanned photos were analysed after completing the binarisation. The surface porosity was presented as a percentage value, which was calculated by dividing the areas of the pixels with value of 1 by that with value of 0. The surface porosity of a particle cross-section was averaged if there were multiple micrographs at the same cross-section. The results of the experiment are shown in Fig. 6.

Surface porosity ratio

The surface porosity ratio e_w, which is usually defined as the ratio of the cross-sectional area of calcareous sand particles with pores, and that without pores, is written as

$$e_w = \frac{G_w}{(G_T - G_W)} \times 100\%$$

where G_w is the cross-sectional area of all pores, and G_T is the total area of the entire region of analysis.

After a similar procedure of surface porosity calculation, the surface porosity ratio was determined though dividing the areas of the pixels with value of 1 by that with value of 0. Again, the surface porosity ratio of a particle cross-section was averaged if there were multiple micrographs at the same cross-section. The results of the experiment are shown in Fig. 7.

As can be seen in Figs. 6 and 7, the surface porosities of particles with pore diameter >2 mm and those in the range of 1–2 mm were 0·66 and 1·07% respectively. The surface porosity ratios of particles with pore diameter >2 mm and those in the range 1–2 mm were 0·67 and 1·08% respectively.

Figures 6 and 7 also show that the surface porosity and surface porosity ratios of the calcareous sand cross-sections were small. However, the surface porosity of particle cross-sections was relatively larger for that of

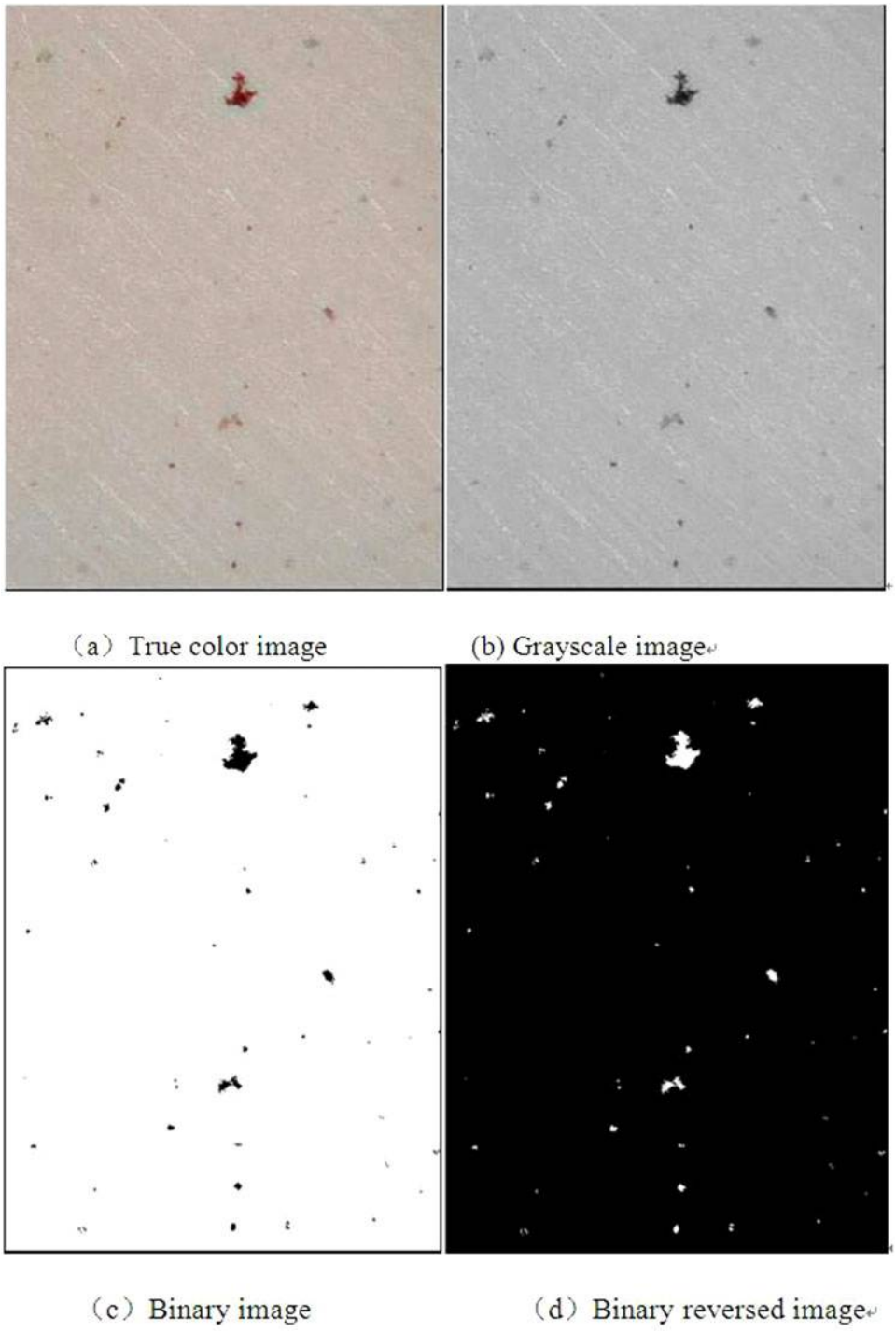

3 Binarisation of micrographs

pore diameter >2 mm, and the difference between particles was larger.

Pore distribution

The identification of all the individual pores and the identification/measurement of their two-dimensional surface areas provide the basis of the pore size distribution analysis. First, pores were classified based on their surface areas, resulting in five levels: $S \leq 1\ \mu m^2$, $1\ \mu m^2 < S \leq 10\ \mu m^2$, $10\ \mu m^2 < S \leq 100\ \mu m^2$, $100\ \mu m^2 < S \leq 1000\ \mu m^2$ and $S > 1000\ \mu m^2$. The micrographs were analysed, and the inner pore sizes were classified based on these five levels. The inner pore distributions in particle cross-sections are shown in Fig. 8 with particle diameter >2 mm and in the range of 1–2 mm.

As can be seen in Fig. 8, for the calcareous sand being tested, inner pores with areas between 10 and 1000 μm^2 occupied >70% of the total area of pores. Furthermore, inner pores with area of 100–1000 μm^2 occupied ~50% of the total area, which was the largest proportion found.

For the calcareous sand particles in the samples with different particle size, the difference in the area distribution was relatively small. For particles >2 mm, the proportion of inner pores with area >1000 μm^2 was only slightly larger than that for particles in the range of 1–2 mm.

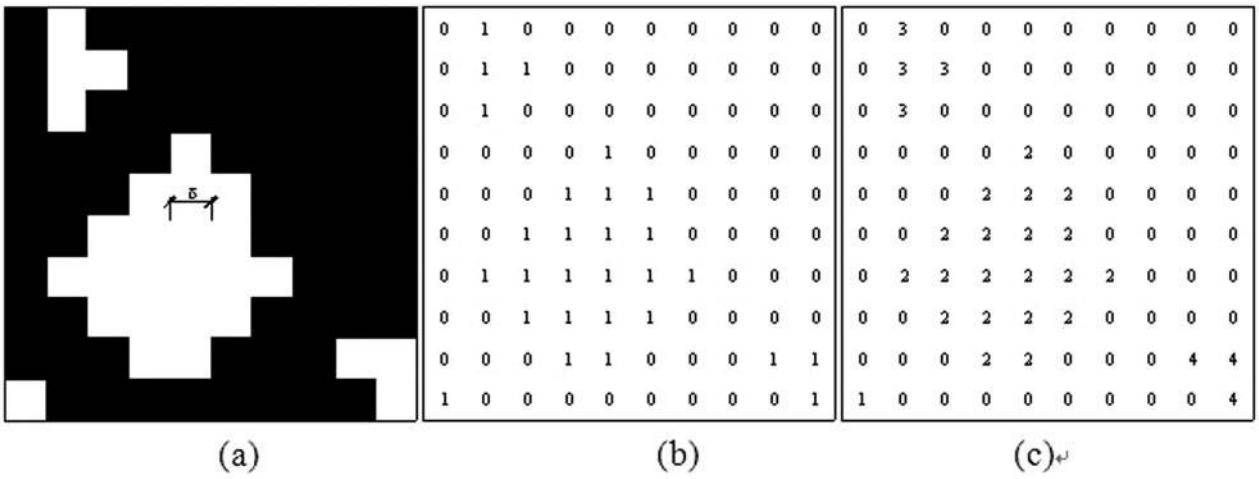

4 Schematic diagram of binarised image storage

However, in our analysis based on the number of inner pores, a different phenomenon was observed in the area distribution, as shown in Fig. 9.

As depicted from Figs. 8 and 9, the pores of the calcareous sand particles with <10% of the total number of pores occupied >70% of the total pore area (10–1000 μm^2). The inner pores with <2% of the total number of pores occupied most of the pore area (~50%; 100–1000 μm^2). Moreover, micropores ($S \leq 1$ μm^2) with >65% of the total number of pores occupied the least area.

From above analysis, there were smaller and fewer larger inner pores, in terms of the number of inner pores for the calcareous sand particles used in this experiment. On the other hand, in terms of the area they constituted, small pores contributed to a small portion of the total pore area, while large pores occupy a much larger portion of the total pore area.

Shape coefficient of pores

Typically, pores in soil media are not spherical in nature, and circular pores were rarely found in the particle cross-sections in the samples. Therefore, the pore diameters cannot be measured in a direct quantitative analysis. Instead, the areas of pores with different shapes were measured to calculate their equivalent diameters. Obviously, the lower the isometric degree of the pore shape, the higher the degree of anisotropy and lower the precision of the equivalent diameter. Thus, the shape of a given pore has direct impacts on the precision of the calculation of its equivalent diameter. Moreover, pore size and geometry can also affect a pore's physical and mechanical properties. Round pores and long strip shaped pores such as cracks clearly have different effects on a rock's mechanical property.

The shape of the inner pores directly affects the crushing behaviour and characteristics of calcareous sand particles. Therefore, analysis of the shape of the inner pores is of great importance in understanding the crushing behaviour of calcareous sand particles. The pore shape coefficient K_f is commonly used in evaluating the shapes of pores. K_f is defined based on the comparison between the pore area of the equivalent

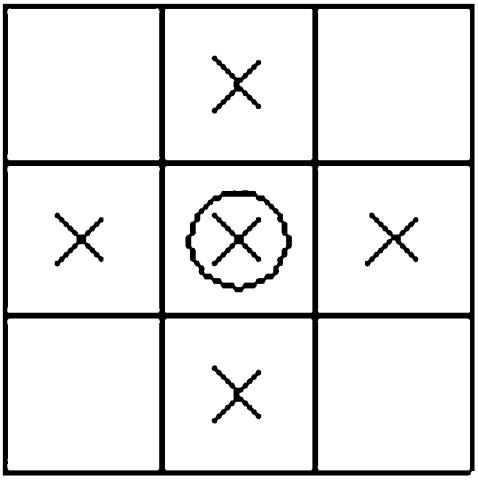

5 Schematic diagram of 'four-neighbourhood' search method

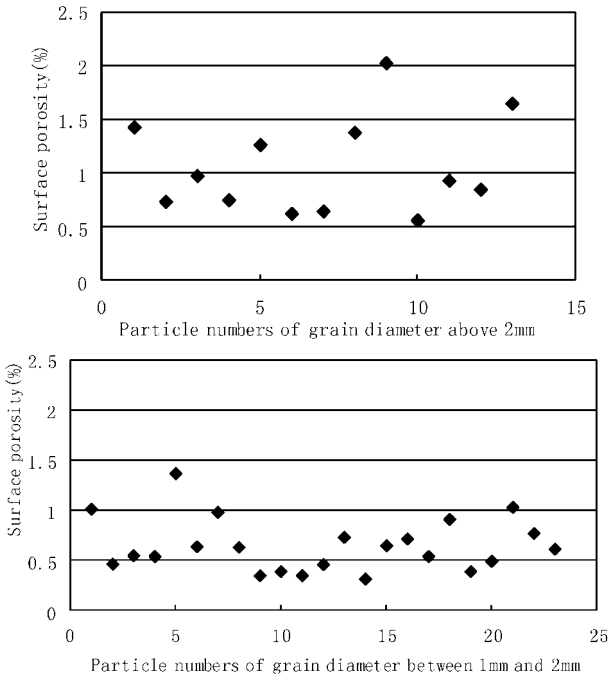

6 Scatter diagram of surface porosity of calcareous sand cross-section

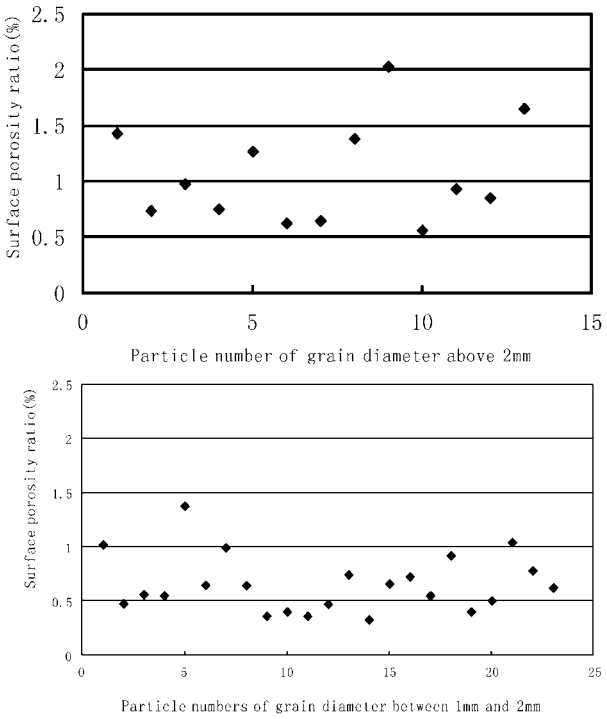

7 Scatter diagrams of surface porosity of calcareous sand cross-section

circumference and that of the actual circumference. The inner pores were measured from the micrographs of particle cross-sections. The area is denoted as S, and the circumference is denoted as P. The equivalent diameter of the pores $D=(4S/\pi)^{1/2}$, and the equivalent circumference was determined as $P_t=\pi D=(4\pi S)^{1/2}$. Thus, K_f can be expressed as follows:

$$K_f=\frac{P_t}{P}=\frac{(4\pi S)^{1/2}}{P}=3{\cdot}545S^{1/2}/P$$

According to this equation, K_f can be used to represent the pore shape. For example, $K_f=1$ represents circular pores; $K_f=0{\cdot}953$ represents square pores; and $K_f=0{\cdot}777$ represents triangular pores.

Based on the isoporosity, pores can be classified into the following three categories:

(i) equiaxed pores: the ratio of the major and minor axes of the pore is $<1{\cdot}5$
(ii) inequiaxed pores: the ratio of the major and minor axes of the pore is between 1·5 and 10
(iii) slit-like pores: the ratio of the major and minor axes of the pore is >10.

From obtained plane images of pores, they often appear as ellipses. If defining a as the major semi-axis of such an ellipse, and b as the minor semi-axis, the pore shape coefficient, K_f, can be expressed as follows

$$K_f=\frac{4(ab)^{1/2}}{3(a+b)-2(ab)^{1/2}}$$

If $a/b=1$, i.e. a circular pore, then $K_f=1$; if $a/b=1{\cdot}5$, then $K_f=0{\cdot}97$; and if $a/b=10$, then $K_f=0{\cdot}47$.

Based on the above analysis, inner pores with $K_f<0{\cdot}47$ were identified as slit-like pores, those with $K_f>0{\cdot}97$ as isometric pores, and the rest as anisometric pores (Table 1).

Using above method, the pore shape analysis of particle cross-sections was performed.

A summary of the inner pore shape coefficients is shown in Fig. 10.

Spherical pores are projected as a shape of circle in two-dimensional planes. Their pore shape coefficient is 1·0. Theoretically, their values cannot be smaller than 1·0. However, as can be seen in Fig. 10, a considerable proportion of the pore shape coefficients were $>1{\cdot}0$. This can be explained as follows. When digitising the micrographs, discontinuity occurs in the resulting images. This effect was particularly obvious for micropores. Because of the limitation of the magnification, the precision of the digitisation of the inner pores was not sufficiently high. Therefore, there were occasional errors in the analysis of micropore shapes. In light of this, it is suggested that for this type of analysis of the micropore shapes, the magnification must be increased to improve the precision of digitisation.

As can be seen in Table 1 and Fig. 10, the difference of the number of inner pores with different shapes was small when the particle sizes were different. In this study, two types of calcareous sand particles were used: diameter >2 mm and diameter between 1 and 2 mm. Less than 2% of the inner pores were slit-like pores, and >98% were equiaxed or inequiaxed pores. Among this,

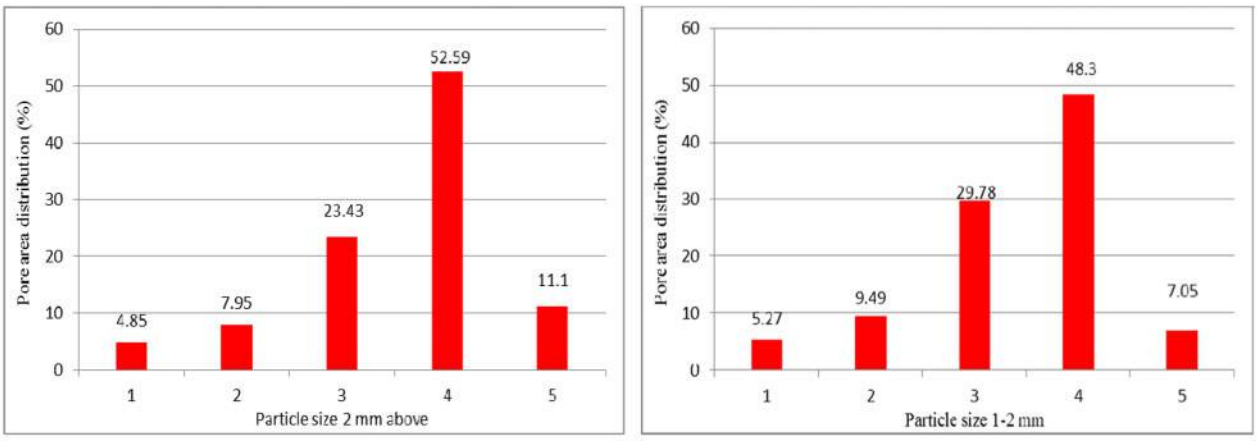

8 Inner pore distribution in particle cross-section

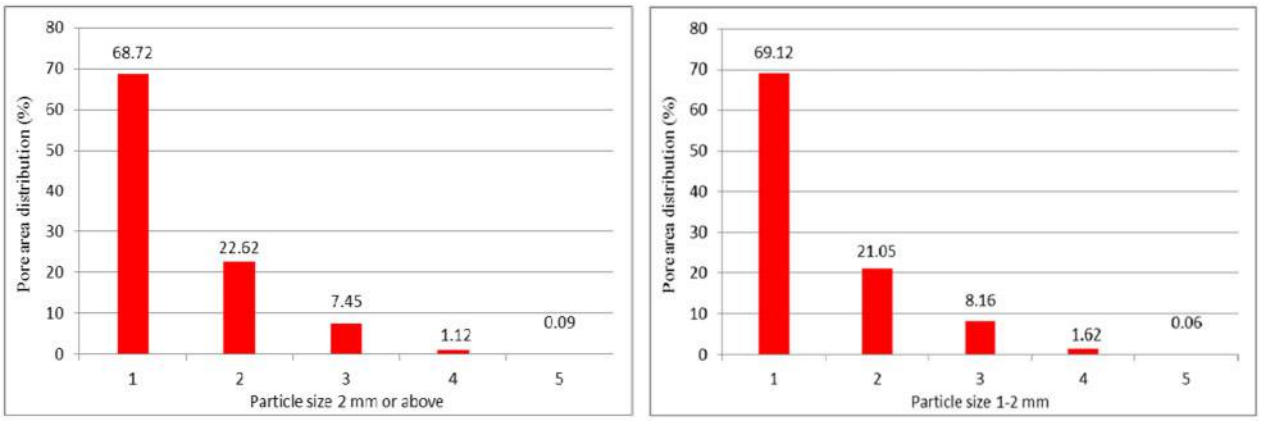

9 Pore number distribution in particle cross-section

>55% of the total number of pores were identified as the equiaxed inner pores.

Discussion and conclusions

Discussion

It is worth mentioning that the image obtained cannot completely reflect the appearance and characteristics of the entire structure, with the microstructural analysis based on the scanned image of a sample cross-section for heterogeneous and anisotropic microstructures. Two mutually perpendicular sections were analysed, which are parallel and perpendicular to the principal direction of variation. For a homogeneous medium, either section can be selected for analysis.

In addition, due to single magnification factor used in this study, the complete information about the pore characteristics in the sample cannot be obtained. Some small pores may not be observed due to limitation of magnification. In order to obtain the complete information about the pores in the samples, different magnification factor should be tested.

In this study, a statistical experimental method was used to analyse the inner pores of calcareous sand. Statistically, it is assumed that the calcareous sand particles were homogenous and isotropic. Thus, any cross-section of the particles could be chosen in the analysis. However, due to the limitations of the experimental conditions, analysis was only performed at a single degree of magnification. Analysis was performed on the size and characteristics of the inner pores of calcareous sand.

Conclusions

In this study, a femtosecond laser cutting method was used to obtain flat cross-sections of calcareous sand particles while maintaining the original morphology of the inner pores. Micrographs of the inner pores of calcareous sand were obtained with a 3D video microscopic visualiser. The image processing toolbox of MATLAB was employed to process the micrographs and analyse the characteristic parameters of the inner pores of calcareous sand. The following conclusions are drawn from the experimental results.

1. The surface porosity was relatively low for calcareous sand particles in the sample. The surface porosity of particles >2 mm and that of particle size between 1 and 2 mm were determined to be 0·66 and 1·07% respectively.

2. For particles with different sizes (in this study, those >2 mm and those in the range of 1–2 mm), the difference in the size distributions of the inner pores was relatively small. Quantitatively, fewer large pores and a greater number of small pores were found. In terms of the total pore area in calcareous sand, small pores occupy a small proportion of the area, while large pores contributed to a larger proportion. Specifically, the inner pores sized between 100 and 1000 μm^2 that occupied the most areas constituted ~50% of the total pore area. Micropores ($S \leq 1$ μm^2) constituted >65% of the total number of pores.

3. The different shapes of inner pores also affect the distribution. Less than 2% of the inner pores were determined to be slit-like shape. More than 98% of the pores are either equiaxed or inequiaxed, with >55% of pores are equiaxed.

Acknowledgements

This study is financially supported by the National Natural Science Foundation of China (grant nos. 41372318 and 51108449), National Program on Key Basic Research Project of China (grant no. 2013-CB956104) and the National Special Program of Science and Technology of China (grant no. 2012FY-112400). The authors also highly appreciate the anonymous reviewers for their critical and helpful comments.

Table 1 Percentage distribution of different pore shapes

	Percentage distribution of different shapes of pores		
Size of sample particles/mm	K_f<0·47	0·47≤K_f≤0·97	K_f>0·97
>2	0·8	37·6	61·6
1–2	1·1	42·4	56·5

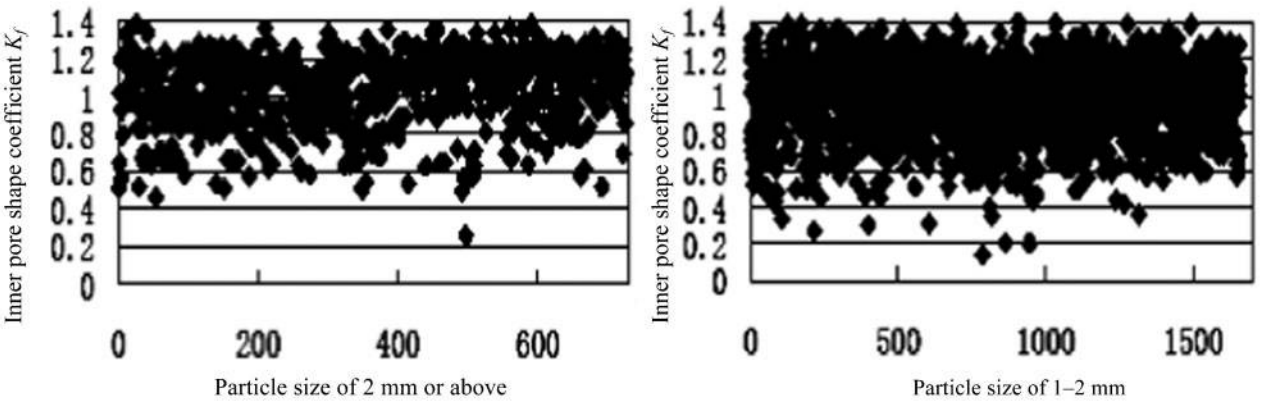

10 Inner pore shape coefficient of particle cross-sections

References

1. H. G. Poulos: 'A review of the behavior and engineering properties of carbonate soils', in 'Engineering properties of calcareous sediments', (ed. H. G. Poulos *et al.*), 17–27; 1990, Sydney, University of Sydney.
2. B. McClelland: 'Calcareous sediments: an engineering enigma', Proc. Int. Conf. ''Calcareous sediments'', Perth WA, Australia, March 1988, 777-784.
3. S. Ohno, H. Ochiai and N. Yasufuku: 'Estimation of pile settlement in calcareous sans', in 'Engineering for calcareous sediments', (ed. K. A. Al-Shafei), 1–6; 1999, Rotterdam, Balkema.
4. H. G. Brandes: 'Simple shear behavior of calcareous and quartz sands', *Geotech. Geol. Eng.*, 2011, **29**, 113–126.
5. H. Shahnazari and R. Rezvani: 'Effective parameters for the particle breakage of calcareous sands: an experimental study', *Eng. Geol.*, 2013, **159**, (12), 98–105.
6. T. S. Hull, H. G. Poulos and H. Alehossein: 'The static behavior of various sediments', in 'Engineering for calcareous sediments', (ed. R. J. Jewell and D. C. Andrews), 59–70; 1988, Rotterdam, Balkema.
7. H. Shahnazari, M. A. Tutunchian, R. Rezvani and F. Valizadeh: 'Evolutionary-based approaches for determining the deviatoric stress of calcareous sands', *Comput. Geosci.*, 2013, **50**, 84–94.
8. Y. Yao and D. Liu: 'Comparison of low-field NMR and mercury intrusion porosimetry in characterizing pore size distributions of coals', *Fuel*, 2012, **95**, 152–158.
9. Q. Zeng, K. Li, T. Fen-Chong and P. Dangla: 'Analysis of pore structure, contact angle and pore entrapment of blended cement pastes from mercury porosimetry data', *Cem. Concr. Compos.*, 2012, **34**, (9), 1053–1060.
10. X.-Z. Wang, Y.-Y. Jiao, R. Wang *et al.*: 'Engineering characteristics of the calcareous sand in Nansha Islands, South China Sea', *Eng. Geol.*, 2011, **120**, 40–47.
11. H. Chen, R. Wang, J. Li and J. Zhang: 'Grain shape analysis of calcareous soil', *Rock Soil Mech.*, 2005, **26**, 1389–1392.